Critical Behaviour in Gravitational Collapse of a Yang-Mills Field

Matthew W. Choptuik

Center for Relativity, The University of Texas at Austin, Austin, TX 78712-1081

Tadeusz Chmaj*

Princeton University Observatory, Princeton, NJ 08544-1001

Piotr Bizoń

Department of Physics, Jagiellonian University, Cracow, Poland
(August 9, 2018)

We present results from a numerical study of spherically-symmetric collapse of a self-gravitating, SU(2) gauge field. Two distinct critical solutions are observed at the threshold of black hole formation. In one case the critical solution is discretely self-similar and black holes of arbitrarily small mass can form. However, in the other instance the critical solution is the $n = 1$ static Bartnik-Mckinnon sphaleron, and black hole formation turns on at finite mass. The transition between these two scenarios is characterized by the superposition of both types of critical behaviour.

04.25.Dm, 04.40.-b, 04.70.Bw

In a recent numerical study of gravitational collapse of a massless scalar field, a type of critical behaviour was found at the threshold of black hole formation [1]. More precisely, in the analysis of spherically-symmetric evolution of various one-parameter families of initial data describing imploding scalar waves, it was observed that there is generically a critical parameter value, $p = p^\star$, which signals the onset of black hole formation. In the subcritical regime, $p < p^\star$, all of the scalar field escapes to infinity leaving flat spacetime behind, while for supercritical evolutions, $p > p^\star$, black holes form with masses well-fit by a scaling law, $M_{BH} \propto (p - p^\star)^\gamma$. Here, the critical exponent, $\gamma \simeq 0.37$, is universal in the sense of being independent of the details of the initial data. Thus, the transition between no-black-hole/black-hole spacetimes may be viewed as a continuous phase transition with the black hole mass playing the role of order parameter. In the intermediate asymptotic regime (i.e. before a solution "decides" whether or not to form a black hole) near-critical evolutions approach a universal attractor, called the critical solution, which exhibits discrete self-similarity (echoing). Using the same basic technique of studying families which "interpolate" between no-black-hole and black-hole spacetimes, similar critical behaviour has been observed in several other models of gravitational collapse [2–4].

In this letter we summarize results from numerical study of the evolution of a self-gravitating non-abelian gauge field modeled by the $SU(2)$ Einstein-Yang-Mills (EYM) equations. In addition to its intrinsic physical interest, we have chosen this model since, in contrast to all previously studied models, it contains static solutions which we suspected could affect the qualitative picture of critical behaviour. Let us recall that these static solutions, discovered by Bartnik and Mckinnon (BK) [5,6], form a countable family X_n ($n \in N$) of spherically-symmetric, asymptotically flat, regular, but unstable, configurations.
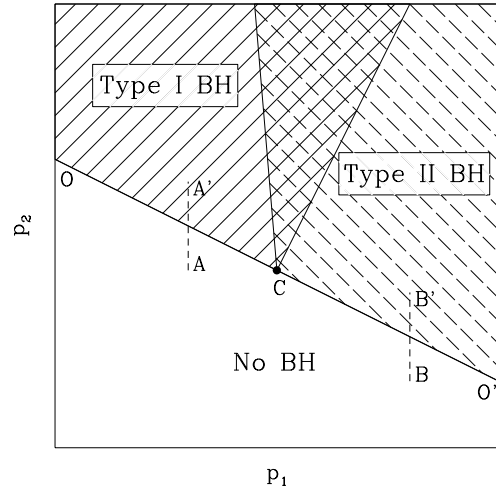

FIG. 1. Schematic representation of "phase-space" for spherically symmetric Yang-Mills collapse, showing possible end states of evolutions from a sufficiently general two-parameter family of initial conditions. The critical line OO' demarks the threshold of black hole formation. An interpolating family such as AA' exhibits Type I behaviour: the critical solution is the static BK solution X_1, and the smallest black hole formed has finite mass. Families such as BB' exhibit Type II behaviour: the critical solution is discretely self-similar ($\Delta \approx 0.74$), black hole formation turns on at infinitesimal mass, and mass-scaling with $\gamma \approx 0.20$ is observed. At C, the two types of critical behaviour coexist.

Our main new result is the observation that for certain families of initial data the static BK solution X_1 plays the role of a critical solution separating collapse from dispersal. Since in this case there is a finite gap in the spectrum of black hole masses, we call this "Type I" behaviour (in

analogy to a first order phase transition), to distinguish it from "Type II" behaviour (which we also observe), where black hole formation turns on at infinitesimal mass. As is shown schematically in Figure 1, sufficiently general two-parameter families of initial data exhibit both types of critical behaviour.

We consider spherically-symmetric Einstein-Yang-Mills equations with the gauge group $SU(2)$. Following [1], we write the general time-dependent, spherically-symmetric metric as

$$ds^2 = -\alpha^2(r,t)dt^2 + a^2(r,t)dr^2 + r^2d\Omega^2. \tag{1}$$

For the YM field we assume the purely magnetic ansatz which in the abelian gauge means that the field strength has the form [7]

$$\dot{W}dt \wedge \Omega + W'dr \wedge \Omega - (1 - W^2)\tau_3 d\vartheta \wedge \sin\vartheta d\varphi, \tag{2}$$

where $\Omega = \tau_1 d\vartheta + \tau_2 \sin\vartheta d\varphi$, τ_i ($i = 1, 2, 3$) are Pauli matrices, an overdot denotes $\partial/\partial t$ and a prime denotes $\partial/\partial r$. Thus the matter content of the model is described by a single function, $W(r,t)$, which we hereafter refer to as the Yang-Mills potential. We note that, as follows from (2), the vacua of the YM field are given by $W = \pm 1$. We introduce auxiliary YM variables, $\Phi \equiv W'$ and $\Pi \equiv a\dot{W}/\alpha$. The dynamics of the EYM model can then be computed using the following set of equations (see [7]):

$$\dot{\Phi} = \left(\frac{\alpha}{a}\Pi\right)', \quad \dot{\Pi} = \left(\frac{\alpha}{a}\Phi\right)' + \frac{\alpha a}{r^2}W\left(1 - W^2\right), \tag{3}$$

$$\frac{a'}{a} = \frac{1 - a^2}{2r} + \frac{1}{r}\left(\Phi^2 + \Pi^2 + \frac{a^2}{2r^2}\left(1 - W^2\right)^2\right), \tag{4}$$

$$\frac{\alpha'}{\alpha} = \frac{a^2 - 1}{2r} + \frac{1}{r}\left(\Phi^2 + \Pi^2 - \frac{a^2}{2r^2}\left(1 - W^2\right)^2\right), \tag{5}$$

$$W(r,t) \equiv \pm 1 + \int_0^r \Phi(\tilde{r}, t)d\tilde{r}. \tag{6}$$

We have solved the initial value problem for many one-parameter families of asymptotically flat, regular initial data, some of which are listed in Table I. To ensure regularity at the origin we require that $W(r,t) \to \pm 1 + O(r^2)$ as $r \to 0$. The numerical results described below were generated using a modified version of the adaptive-mesh algorithm used to perform the original scalar field calculations [1]. The sensitivity of the mesh-refinement algorithm was again very helpful in efficiently computing near-critical solutions, but was not nearly as crucial as it was for the scalar case. In fact, we have also reproduced most of the following results using a uniform-grid code much like the one described in [8].

As stated above, depending on the particular form of initial data used, we have found two types of critical behaviour:
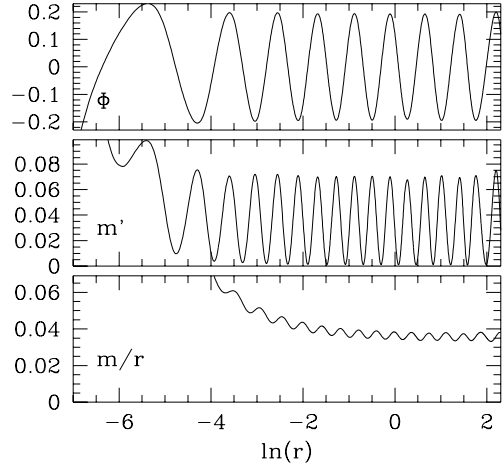

FIG. 2. Late time profiles of marginally subcritical Type II collapse using family (a) (see Table 1). Note that the mass aspect, $m(r,t)$, is defined via $a^2 = (1 - 2m/r)^{-1}$. The large number of echoes visible here (for fixed $|p-p^\star|/p^\star$), relative to the scalar case, is a reflection of the relatively small value of the echoing exponent ($\Delta_{\mathrm{YM}} \approx 0.74$ versus $\Delta_{\mathrm{SF}} \approx 3.44$). However, this is partly offset by the fact that the mass-scaling exponents for the two models also differ significantly. In general, dimensional/scaling considerations suggest that $\Delta\delta n = -\gamma\delta\pi$ where δn and $\delta\pi$ are the changes in echo number, n, and $\pi \equiv \ln|p - p^\star|$, respectively [17].

Type II behaviour.—In this case we observe a continuous no-black-hole/black-hole phase transition, and the overall picture of criticality is very much analogous to that of scalar field collapse. For a generic Type II family, and in the near-critical, non-linear regime, we conjecture that the evolution asymptotes to a locally unique (up to $r, t \to \sigma r, \sigma t$, for arbitrary $\sigma > 0$) discretely self-similar solution, with an echoing exponent, $\Delta \approx 0.74$. As with the scalar field case, we expect that the precisely critical solution echos an infinite number of times, exhibits unbounded growth of curvature near $r = 0$, and is singular at the origin at some finite value of central proper time, $T^\star$. Figure 2 show profiles of various echoing quantities at $T \approx T^\star$ from a family (a) calculation (see Table I) with $|s - s^\star|/s^\star \approx 10^{-15}$. Typical evidence for scale-periodicity is shown in Figure 3, using near-critical data from family (b) with parameter a varying. The level of agreement between the two independently computed estimates of Δ provides us with a rough measure of the accuracy of our computation of the exponent.

As expected, Type II families also exhibit mass-scaling in the super-critical regime: $M_{BH} \propto (p - p^\star)^\gamma$. Typical results are shown in Figure 4 and we estimate that the value $\gamma \approx 0.20$ is accurate to a few percent. We note in passing that this result is another piece of the growing body of evidence which has shown that γ is *not* constant across all collapse models [9,4,10]. As argued in [11], mass-scaling and universality (initial-data-

independence), strongly suggest that the stable manifold of a Type II solution, such as the one described here, is of codimension one. This picture, which predicts that γ is the reciprocal of the Lyapounov exponent of a single growing mode associated with a critical solution, has now been validated for at least two distinct matter models with *continuously* self-similar critical solutions [11,12,4,13,14]. Perturbative treatment of critical solutions with discrete symmetry is more involved, although considerable progress has been made for the scalar case [15]. Here we only remark that any techniques which work for the scalar field should be largely applicable to this solution.
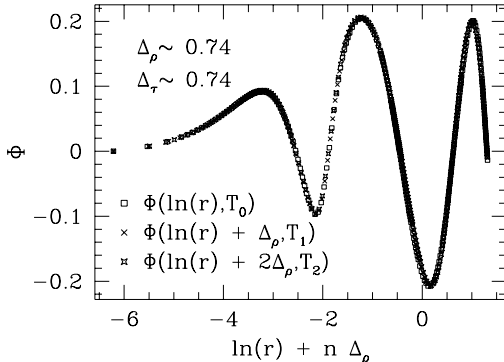

FIG. 3. Illustration of scale-periodicity of Type II solution. This plot shows the superposition of a near-critical profile of Φ (at a particular time) with the first two echoes which subsequently develop. The central proper time, T_0, at which the earliest profile is monitored is arbitrary; times T_1 and T_2 and the rescaling exponent, Δ_ρ, are then chosen to minimize $\Phi(\ln(r)+n\Delta_\rho, T_n) - \Phi(\ln(r), T_0)$. An independent estimate of Δ is generated by first estimating the critical time, $T^\star$ for the family, and then computing $\Delta_\tau \equiv \ln((T^\star - T_n)/(T^\star - T_{n+1}))$.

Type I behaviour.—As stated previously, solutions in a Type I interpolating family asymptote to the *static* BK solution X_1 as $p \to p^\star$. This behaviour appears generically for kink-type initial profiles of the YM potential W, such as family (c) in Table I. In this case it has already been established that the each of the BK solutions, X_n, has exactly n unstable modes (within the ansatz (2)); hence we are certain that the stable manifold of the critical solution has codimension one. Initial data with small $|p - p^\star|$ results in an evolution which approaches X_1 and stays in its vicinity for central proper time, $T \approx -\lambda \ln |p - p^\star|$. The configuration then either disperses to infinity ($p < p^\star$) or collapses to a black hole with finite mass ($p > p^\star$). Typical results from a marginally subcritical Type I evolution are shown in Figure 5.

Our calculations are somewhat complementary to those performed by Zhou and Straumann [8]. Those authors generally used initial conditions describing small deviations from the static solution X_1, and studied the subsequent evolution to verify the prediction of perturbative instability of X_1 [16]. Here, by construction, we *generate* the solution X_1 as the boundary between collapse and dispersal, and thus immediately verify its instability. In this case, the reciprocal Lyapounov exponent of the single unstable mode yields the characteristic time scale, λ, for the decay of X_1. Using central-proper-time normalization, the value computed from perturbation theory [16] is $\lambda = 0.5519\ldots$.
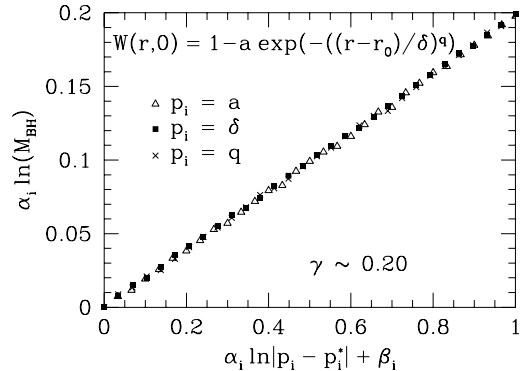

FIG. 4. Mass-scaling of Type II solutions. Each marker type corresponds to a different family of super-critical computations. For each family, constants α_i and β_i are chosen to unit-normalize the x-range and place the first data-point (smallest black hole) at the origin. For all plots, the least squares fit for the slope, γ, is 0.20, with an estimated uncertainty of a few percent. In addition, for all families, the unnormalized π range was 18; thus in each case, the black hole mass spans a factor of $e^{18\gamma} \approx 37$.

We can measure this exponent quite directly from our simulations by computing the variation of the lifetime of near-critical solutions with respect to variations in $\pi \equiv \ln |p - p^\star|$. Specifically, defining $T_r(\pi)$ to be the central proper time at which the zero-crossing of $W(r,t)$ reaches radius r as it propagates outwards, we expect $-dT_r/d\pi \to \lambda$ as $\pi \to -\infty$ and for sufficiently large r. Some numerical regularization is provided by monitoring T_r at several discrete radii $r_i, i = 1\ldots n$ and computing the averaged quantity $\bar{T}_r(\pi) \equiv n^{-1}\sum T_{r_i}(\pi)$. When this is done for family (c) with $r_1 = 400, r_n = 475, n = 16$, we find $0.5525 < -d\bar{T}_r/d\pi < 0.5520$ for $-19 < \pi < -10$. In addition, we can get a good estimate of the unstable *eigenmode* by studying near-critical departures from the static solution.

As noted in the introduction, Type I behaviour is clearly characterized by a gap in the black hole mass spectrum at threshold. We conjecture that the mass-gap is universal, and observe that our calculations suggest that it is very close (1% or less) to the total mass of the static solution ($m_1 = 0.828640\ldots$).

Type I and II coexistence.—We can only briefly describe what is one of the more interesting features of critical behaviour in the EYM model: the fact that for

certain two parameter families—such as (a) and (d) in Table I—there exists a critical line in parameter space (see Fig 1) which interpolates between Type I and Type II behaviour. The results we have obtained lead us to conjecture that the transition point (C in Fig 1) represents coexistence of the two distinct critical solutions described above. In other words, near C, we see echoing occurring in context of the static, $n = 1$ background. Thus we can have have arbitrarily small black hole formation within a configuration which itself is arbitrarily close to forming a finite-mass black hole. We end by noting that the super-critical regime in this model, especially in the cross-hatched overlap region sketched in Fig 1 is still very much *terra incognita*, although we have preliminary evidence that further phenomenological richness lurks there. In particular, we have observed there an intriguing discontinuity in the spectrum of black-hole masses, which suggests the existence of another type of critical behaviour in the formation of black holes [18].
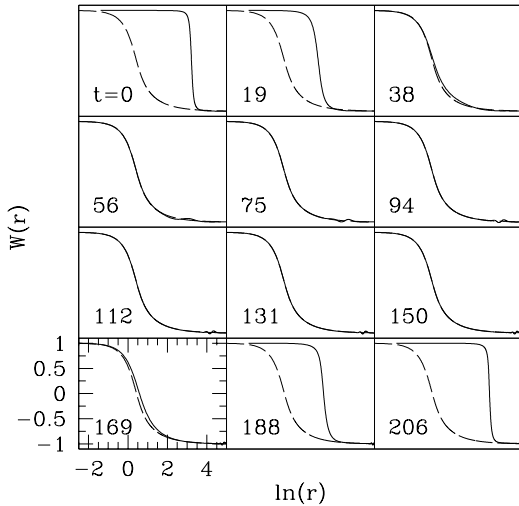
FIG. 5. Marginally subcritical Type I evolution. Here we plot the dynamical evolution of $W(r, t)$ (solid line) and superimpose the static BM configuration X_1 (dashed line). Initially, the evolution (family (c), $|\delta - \delta^\star|/\delta^\star \approx 10^{-15}$) is nearly linear and almost purely ingoing. When the pulse arrives at the center, it sheds off YM radiation, approaches X_1 and stays near it for some time, and then disperses to infinity.

[*] Kosciuszko Foundation Fellow. On leave of absence from N. Copernicus Astronomical Center, Cracow, Poland.
[1] M. W. Choptuik, Phys. Rev. Lett. **70**, 9-12 (1993).
[2] A.M. Abrahams and C.R. Evans, Phys. Rev. Lett. **70**, 2980-2983 (1993).
[3] C.R. Evans, and J.S. Coleman, Phys. Rev. Lett. **72**, 1782-1785 (1994).
[4] R. S.Hamade, J. H. Horne, and J. M. Stewart, LANL preprint gr-qc/9511024 (1995).
[5] R. Bartnik and J. Mckinnon, Phys. Rev. Lett. **61**, 141 (1988).
[6] J. A. Smoller and A. Wasserman, Commun. Math. Phys. **151**, 303 (1993).
[7] R. Bartnik, Proceedings of the Third Hungarian Relativity Workshop, ed. Z. Perjes (Budapest, World Scientific, 1990).
[8] Z.-H. Zhou and N. Straumann, Nucl. Phys. **B360**, 180 (1991); Z. Zhou, Helv. Phys. Acta. **65**, 767-819 (1992).
[9] D. Maison, Phys. Lett. **B366**, 82-84, (1996).
[10] M W. Choptuik and S. L. Liebling, in preparation, (1996).
[11] T. Koike, T. Hara and S. Adachi, Phys. Rev. Lett. **74**, 5170-5173 (1995).
[12] D. Eardley, E. Hirschmann and J. Horne, Phys. Rev. **D52**, 5397-5401 (1995).
[13] E. Hirschmann and D. Eardley, Phys. Rev. **D52**, 5850-5856 (1995).
[14] E. W. Hirschmann and D. M. Eardley, LANL preprint gr-qc/9511052 (1995).
[15] C. Gundlach, Phys. Rev. Lett. **75**, 3214-3217 (1995).
[16] N. Straumann and Z.-H. Zhou, Phys. Lett. **B243**, 33 (1990).
[17] C. Evans, personal communication, (1993)
[18] P. Bizoń, T. Chmaj and Z. Tabor in preparation, (1996).

4

TABLE I. Initial data families used in the calculations reported here. Listed are the family label, the form of the initial profile, $W(r,0)$, family parameters, p_i, nature of W's initial time derivative, and which behaviour is found by generating interpolating families. Initial data for family (a) is time-symmetric ($\dot{W}(r,0) = 0$); for all other families the initial configurations are almost purely ingoing. Finally, for family (a), the constants a and b are chosen so that $W(0,0) = 1$ and $W'(0,0) = 0$.

Family	$W(r,0)$	p_i	$\dot{W}(r,0)$	Behaviour
(a)	$(1 + a\,(1 + br/s)\exp(-2(r/s)^2))\tanh((x-r)/s)$	x, s	0	I, II
(b)	$1 + a\exp(-((r-20)/\delta)^q)$	a, δ, q	$W'(r,0)$	II
(c)	$(1 - (r/\delta)^2)/((1 - (r/\delta)^2)^2 + 4r^2)^{1/2}$	δ	$W'(r,0)$	I
(d)	$-1 + 2a\exp(-((r-17)/4)^q)$	q, a	$W'(r,0)$	I, II